



OPEN ACCESS

EDITED BY

George Kontakiotis,
National and Kapodistrian University of
Athens, Greece

REVIEWED BY

Yong Zhou,
China University of Petroleum, China
Juye Shi,
China University of Geosciences, China

*CORRESPONDENCE

Yuanyuan Zhang,
✉ yy-zhang@pku.edu.cn

RECEIVED 31 May 2023

ACCEPTED 21 June 2023

PUBLISHED 05 July 2023

CITATION

Tang Y, He W, Wang R, Ren H, Jin Z,
Yang Z and Zhang Y (2023),
Cyclostratigraphy of Lower Permian
alkaline lacustrine deposits in the Mahu
Sag, Junggar basin and its
stratigraphic implication.
Front. Earth Sci. 11:1232418.
doi: 10.3389/feart.2023.1232418

COPYRIGHT

© 2023 Tang, He, Wang, Ren, Jin, Yang
and Zhang. This is an open-access article
distributed under the terms of the
[Creative Commons Attribution License
\(CC BY\)](https://creativecommons.org/licenses/by/4.0/). The use, distribution or
reproduction in other forums is
permitted, provided the original author(s)
and the copyright owner(s) are credited
and that the original publication in this
journal is cited, in accordance with
accepted academic practice. No use,
distribution or reproduction is permitted
which does not comply with these terms.

Cyclostratigraphy of Lower Permian alkaline lacustrine deposits in the Mahu Sag, Junggar basin and its stratigraphic implication

Yong Tang¹, Wenjun He¹, Ran Wang¹, Haijiao Ren¹, Zhijun Jin²,
Zhuang Yang^{2,3} and Yuanyuan Zhang^{2,3*}

¹PetroChina Xinjiang Oilfield Company, Karamay, Xinjiang, China, ²Institute of Energy, Peking University, Beijing, China, ³School of Earth and Space Sciences, Peking University, Beijing, China

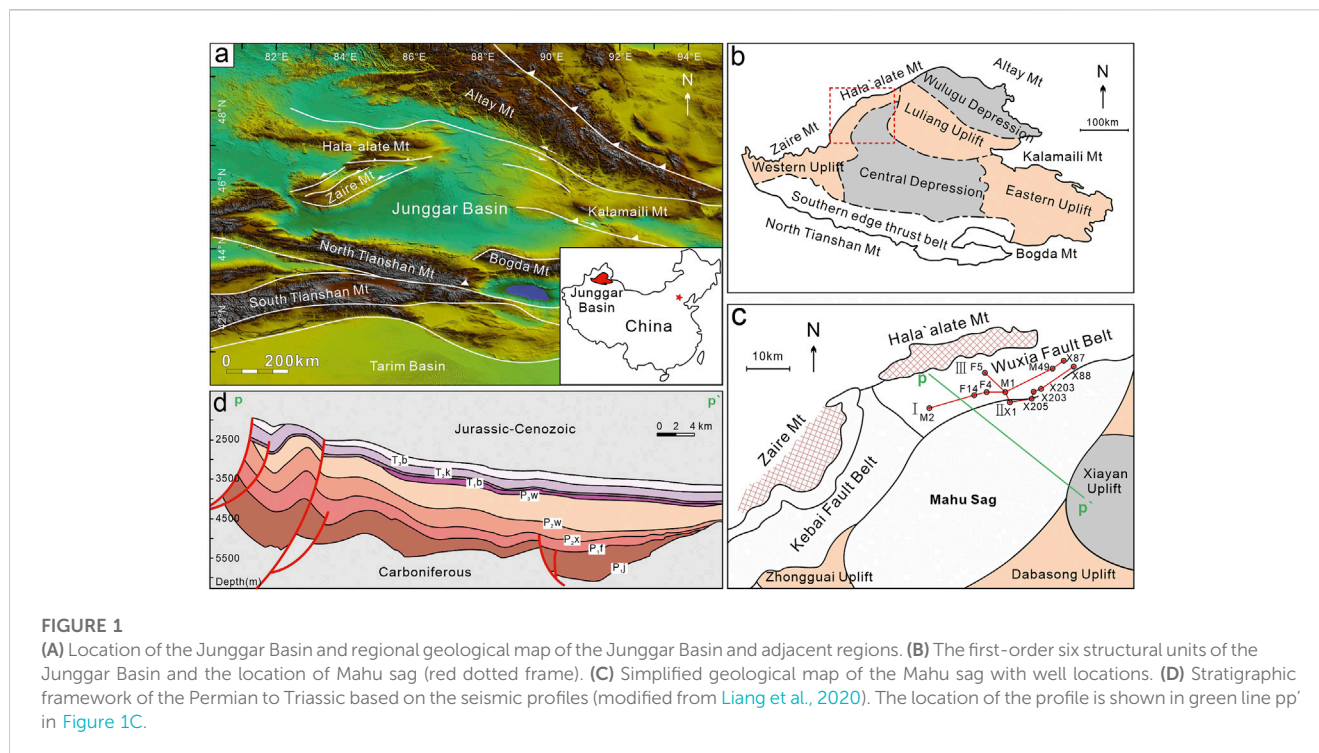
The Lower Permian Fengcheng Formation of the Mahu Sag is one of the most potentially petroliferous sequences in China, and its unique alkaline lacustrine deposits provide important information on the paleoclimate and paleoenvironment of the early Permian. However, because of the complexity of the heterogeneous lithology and sedimentary facies in lacustrine deposits, the lateral correlation of lithofacies becomes challenging. Using cyclostratigraphy, we conducted a detailed astronomical cycle analysis of the Lower Permian Fengcheng Formation in the northern Mahu Sag, established an astronomical time scale, and constructed an isochronous sedimentary framework by collating the cycles of the different wells. Nine 405-kyr long-eccentricity cycles in the Fengcheng Formation were identified, and absolute astronomical time scales were established with the anchored point at ~300 Ma in the Lower member of the Fengcheng Formation. Based on the identification of lithofacies, the spatio-temporal variation in the lithofacies within the Fengcheng Formation was reconstructed. The astronomical time scale has proven to be reliable, and the lithofacies distribution within the isochronal framework is effective for investigating the spatial variation of lithofacies in alkaline lacustrine deposits. Favorable dolomitic mudstones developed in the central and transitional zones, corresponding to the three long-eccentricity cycles in the middle member of the Fengcheng Formation. Tuffaceous mudstones with high potential mainly developed in the lower member of the Fengcheng Formation in the marginal zone of the Mahu Sag. This study demonstrates an approach that can be used to study lithofacies in lacustrine deposits.

KEYWORDS

Fengcheng Formation, lacustrine deposit, cyclostratigraphy, lithofacies identification, isochronal framework

1 Introduction

With its great exploration potential, lacustrine shale oil has been considered a critical strategic target for increasing hydrocarbon production in China (Jin et al., 2021). Shale oil exploration is primarily associated with saline or brackish lacustrine basins (Hu et al., 2022). Alkaline lacustrine deposits develop in extremely salinized lakes and are prone to host high-



quality oil shales (Zhi et al., 2019; Tang Y et al., 2021). The formation of such an alkaline lake is jointly controlled by favorable paleoclimatic, paleotectonic, and paleogeographic conditions (Cao et al., 2020). Alkaline lakes have been proven to be favorable environments for organic matter accumulation and preservation and have been recognized as having high hydrocarbon (Burton et al., 2014; Xia et al., 2022). Therefore, alkaline lacustrine deposits are of great environmental and economic significance in paleoclimatic reconstruction and shale oil exploration (e.g., Smith and Carroll, 2015; Yu et al., 2019) and are characterized by the deposition of alkaline minerals (sodium carbonate minerals) and fine-grained organic-rich sediments (Warren, 2010; Pecoraino et al., 2015). However, the joint controlling factors in the formation of alkaline lakes, rapid facies changes, and variable depositional processes complicate the lithofacies in alkaline lakes, making it challenging to determine the distribution of favorable lithofacies (Li et al., 2019b).

Most known alkaline lake deposits are Eocene or younger in age (Warren, 2010; Wang T et al., 2020), whereas the Lower Permian Fengcheng Formation of the Junggar Basin is the most ancient well-preserved alkaline lacustrine deposit, which recorded crucial paleoclimate information of the Permian era and is considered a favorable archive of the Late Pale Ice Age (LPIA) (Montañez and Poulsen, 2013; Cao et al., 2020). Understanding the distribution of lithofacies in the Fengcheng Formation is fundamental for further paleoclimatic studies. The lack of an isochronal lithofacies framework hinders the lateral lithofacies correlation. Astronomical analysis of sedimentary sequences has been applied widely to find global signals recorded in strata and investigate the sedimentary responses to paleoclimate change of astronomy forcing, based on the Milankovitch theory (Hinnov, 2000; Hinnov, 2013; Sha et al., 2015), in order to establish the isochronal framework. Recently, ~405 kyr long-eccentricity cycles were recognized in the

Late Permian strata (Huang et al., 2020), extending the astronomical time scale to the Paleozoic era.

In this study, we aimed to establish an astronomical time scale (ATS) for targeted sequences of the Fengcheng Formation and to reconstruct the sedimentary isochronal framework of the Fengcheng Formation in the Mahu Sag by lateral comparison among different wells. In combination with lithofacies identification, this study explored the lithofacies distribution of the alkaline lacustrine Fengcheng Formation in northern Mahu Sag, demonstrating an approach that can be used for the study of lithofacies in lacustrine deposits.

2 Geological background

Located in northwestern China, covering an area of approximately 134,000 km², the triangular-shaped Junggar Basin is a large petroliferous superimposed basin, in the southern part of the Central Asian Orogenic Belt (CAOB), which is bounded by the Altay Mountain (Mt.) to the north, the Kalamaili Mt. to the east, the Zaire-Hala'alate Mts. at the northwestern margin, and the North Tianshan-Bogda Mts. to the south (Figure 1A). As an intraplate superimposed basin, the Junggar Basin has experienced multistage intraplate deformation after the final amalgamation of the Paleo-Asian Ocean (PAO) (Zhang et al., 2013; Han and Zhao, 2018; Liu et al., 2017, 2019; Zhang et al., 2016). The Junggar Basin consists of six first-order structural units: Wulugu Depression, Luliang Uplift, Central Depression, West Junggar, Northern Tianshan Overthrust Belt, and East Uplift (Figure 1B). The Mahu Sag is located in the northwestern region of the Central Depression (Figure 1C) and is surrounded by the Zhongguai and Dabasong Uplifts to the south and the Zaire and Hala'alate mountains in the northwest margin,

along which form three NE-SW trending dextral strike-slip faults (Yu et al., 2016; Tang W et al., 2021).

The Mahu Sag developed on the basement of a Paleozoic remnant ocean basin in West Junggar, and the filling process of the remnant ocean basin lasted until the Late Carboniferous (Chen et al., 2013). With the closure of the remnant ocean, the Mahu Sag transformed from marine to terrestrial sedimentation (Li et al., 2015) and evolved into a rift basin during the Permian (Tang W et al., 2021) (Figure 1D). The Lower Permian Fengcheng Formation of the Mahu Sag is considered an ancient alkaline lacustrine deposit (Cao et al., 2015) and has been demonstrated to be a set of fan-lacustrine sedimentary systems (Tang W et al., 2021). With thinning to the southeast (Figure 1D), the Fengcheng Formation is divided into three members with different lithological associations from bottom to top. The lower member (P_1f_1) is transitional with underlying volcanic units, dominated by dark gray mudstone, but contains a few tuffaceous mudstones and mafic-intermediate volcanic rocks. The middle member (P_1f_2) is characterized by alternating beds of evaporite and dolomitic mudstone and contains parts of other lithofacies, such as calcareous mudstone and dolomitic siltstone. Evaporites are dominated by sodium carbonates, which are formed under extremely alkaline water conditions (Yu et al., 2018; Jiang et al., 2023). The upper member (P_1f_3) is dominated by alternating beds of mudstone and siltstone, representing a phase in which salinity decreases and the input of terrestrial detrital sediments gradually increases, following the middle member (Yu et al., 2018; Wang T et al., 2020; Guo et al., 2021).

The Fengcheng Formation in the Mahu Sag is divided into three lateral areas (Cao et al., 2020; Ni et al., 2023), namely, a central zone with substantial deposition of sodium carbonate minerals and dolomitic mudstone, a transitional zone dominated by alternating dolomitic mudstone and siltstone, and a marginal zone dominated by siltstone and coarser sandstone, and quite a few volcanics, which correspond to the lateral changes of the fan-lacustrine sedimentary system.

3 Data and methods

3.1 Logging data

A number of geophysical log series have been utilized in the effort to recover long, continuous, and high-resolution stratigraphy signals (Hinnov, 2000; Li et al., 2019a). Natural Gamma Ray (NGR) logging data have been widely applied in sedimentology and stratigraphy, based on the radiogenic isotope uranium, thorium, and potassium content within sediments. Generally, K consists of minerals such as clays, mica, and feldspar; U and Th commonly exist in minerals such as clays, feldspar, and several heavy minerals; and U is also relatively concentrated in organic matter (Schnyder et al., 2006; Wang M et al., 2020). A high GR is generally attributed to fine-grained facies, such as mudstone and siltstone, whereas a low GR is related to coarser facies such as sandstone (Cantalejo and Pickering, 2015; Li et al., 2019a). Because all the above are associated with relative clay abundance, which is sensitive to environmental and climatic change, NGR log data of outcrops and drill wells are valuable tools for cyclostratigraphy and effective proxies for

paleoclimate analysis (Huang et al., 2021). In addition, caliper and resistivity well logging data were utilized to assist in lithologic identification due to the different intrinsic physical and electric features of sodium carbonates and common rock-forming minerals.

In this study, the NGR profiles of the Fengcheng Formation from four wells, M1, F4, X202, and X203, in the northern Mahu Sag were used to conduct cyclostratigraphy analysis. Stratigraphic cyclicity and paleoclimate quasi-periodicity changes of astronomical forcing could be recognized, horizontal comparison of the astronomical time scale (ATS) performed, and even the establishment of a sedimentary isochronal framework of the whole sag could be conducted. Among the four wells, M1 and F4 were close to each other and approached to the depocenter, and X202 and X203 were close to the lake margin (Figure 1C). The vertical thickness of the four well profiles of the Fengcheng Formation was approximately 300–400 m, and the sampling rate of all the NGR profiles was 0.125 m. Then logging data from 12 wells widespread in the northern the Mahu Sag were used for lithological identification, from which three lateral profiles of the Fengcheng Formation were established in this study.

3.2 Time series analysis methods

Firstly, raw NGR data was screened from the perturbation of events and detrended. Then the spectral analysis of the detrended NGR was conducted to find periodic or quasi-periodic components. The data series in the depth domain were transformed into time domain by astronomical tuning in order to extract potential 405-kyr eccentricity cycles.

3.2.1 Pretreatment of raw NGR data

Climate proxy variations consist of long-terms, 10^3 – 10^6 year-scale orbital (eccentricity, obliquity, and precession) cycles, in addition to being punctuated by isolated events of sedimentary perturbation, such as storm, flooding, and volcanism, so-called sedimentary noises (Hinnov, 2013; Li et al., 2018a), which are more intense and frequent in lacustrine than marine. Therefore, quantitative cyclostratigraphic analysis should differentiate astronomical signals from spectral noise (Huang et al., 2020). Before the time series analysis, obvious isolated event perturbations were removed from the raw NGR data. Volcanism was the most widespread sedimentary perturbation event in the Fengcheng Formation of the northern Mahu Sag, particularly in M1, X202, and X203. Tuff layers and tuffaceous mudstone, characterized by their unusually high NGR values, were recorded in the sections, resulting in the prominent deviations in time series analysis. Then the screened NGR data from the Fengcheng Formation were detrended by subtracting a 35% weighted average to remove long-term trends (Li et al., 2019a).

3.2.2 Spectral analysis and tuning

Spectral analysis is primarily used to recognize periodic or quasi-periodic components in a data series (Li et al., 2019a). Prior to analysis, the NGR data were analyzed using multi-taper method (MTM) spectral estimator with robust red noise models, which could achieve an optimal trade-off between frequency resolution

TABLE 1 Summary of criterion of the identification of lithofacies based on the logging data (adapted from Qian et al. (2022)).

CAL	NGR	Rt	CNL	Litho
<10	>69	15<Rt<80	>0.16	Calcareous Mudstone
	>69	80<Rt<1500	>0.16	Dolomitic Mudstone
	100 ≤ Gr ≤ 130	Rt<80	<0.16	Dolomitic Mudstone
	<69	Rt<15	>0.16	Silty Mudstone
	>69	Rt<15	>0.16	Mudstone
		>1500	0.09<CNL<0.16	Muddy Dolomite
	<130	1500<Rt<2000	<0.09	Silty Dolomite
		>2000	<0.09	Dolomite
	<69	15<Rt<80	>0.16	Calcareous Siltstone
	<100	Rt<80	<0.16	Calcareous Siltstone
	<69	80<Rt<1500	>0.16	Dolomitic Siltstone
		<80	<0.16	Siltstone
		>150		Tuffaceous Mudstone
>10	>69	>1500	>0.09	Sodium carbonate-bearing Mudstone
	<69	>1500	>0.09	Sodium carbonate-bearing Mudstone
>16			>0.3	Sodium Carbonate

and statistical confidence for uniformly spaced time series. Evolutionary spectral analysis was applied to the NGR data to detect the evolution of frequencies through succession, by setting a specific sliding window and a step to detect the targeted frequencies according to the spectral characteristics of the well. Filtering is an efficient way to isolate specific frequency components (according to the results of spectral analysis) in a data series, and frequencies with high significance levels may be related to Milankovitch forcing frequencies. All analysis steps were conducted using *Acycle v2.0* software (Li et al., 2019a). Astronomical tuning is a necessary step when original data, usually in the depth domain, must be transformed into the time domain. A filter signal from the data series can be used to reconstruct the age model by assigning the maximum (or minimum) depth of each filtered series to a time value that is generally obtained from radioisotopic dating (Li et al., 2019a). The absolute astronomical time scale was constructed by anchoring the floating ATS to the U-Pb age of widespread volcanic rocks in the lower member of the Fengcheng Formation at ~300 Ma (Li et al., 2023), which was taken as the anchored point for the absolute time scale in this study.

3.2.3 Evolutional correlation coefficient

The *Acycle v2.0* software includes tools for simultaneously testing the astronomical forcing of paleoclimate data series and mean sedimentation rate with a correlation coefficient (COCO) approach, with an extension for testing the evolution of the sedimentation rate (eCOCO) along the data series (Li et al., 2018b; Li et al., 2019a). The NGR data were analyzed using the COCO approach to find the most likely sedimentation rate and the eCOCO approach to test the evolution of the sedimentation rate

along the data series with a given sliding window and step. ρ (correlation coefficient), H_0 significance level, and number of contributing astronomical frequencies are three key indices for evaluating the availability and significance level of the simulated results (Li et al., 2018b). The sedimentation rate most likely corresponded to the highest correlation coefficient (ρ). A null hypothesis (H_0), that no astronomical frequencies existed, was adopted in the data series, which helped determine whether astronomical forcing existed (Li et al., 2018b). All analysis steps were conducted using *Acycle v2.0* software (Li et al., 2019a).

3.3 Lithofacies identification based on logs data

Based on the log data and drill core samples, lithofacies' identification was performed for 12 wells (Figure 1C). We summarized the distinct lithofacies of the Fengcheng Formation based on the different characteristics of the logging data. Combined with a previous study (Qian et al., 2022), there are three remarkable indices from the logging data to distinguish several different lithofacies (Table 1). 1) Caliper (CAL) is a log index used to measure the size change of the borehole. In general, rocks of different physical natures respond differently to the pressure generated from drilling and the breakout of the well wall increasing in size, whereas the standard borehole size is approximately 9 cm. In the Fengcheng Formation, lithofacies bearing sodium carbonate minerals have a prominent feature: the caliper (CAL) log index is higher than 9, which distinguishes it from other lithofacies. 2) Natural Gamma Ray (NGR) is a reliable index for detecting clay content in different lithofacies, which can help

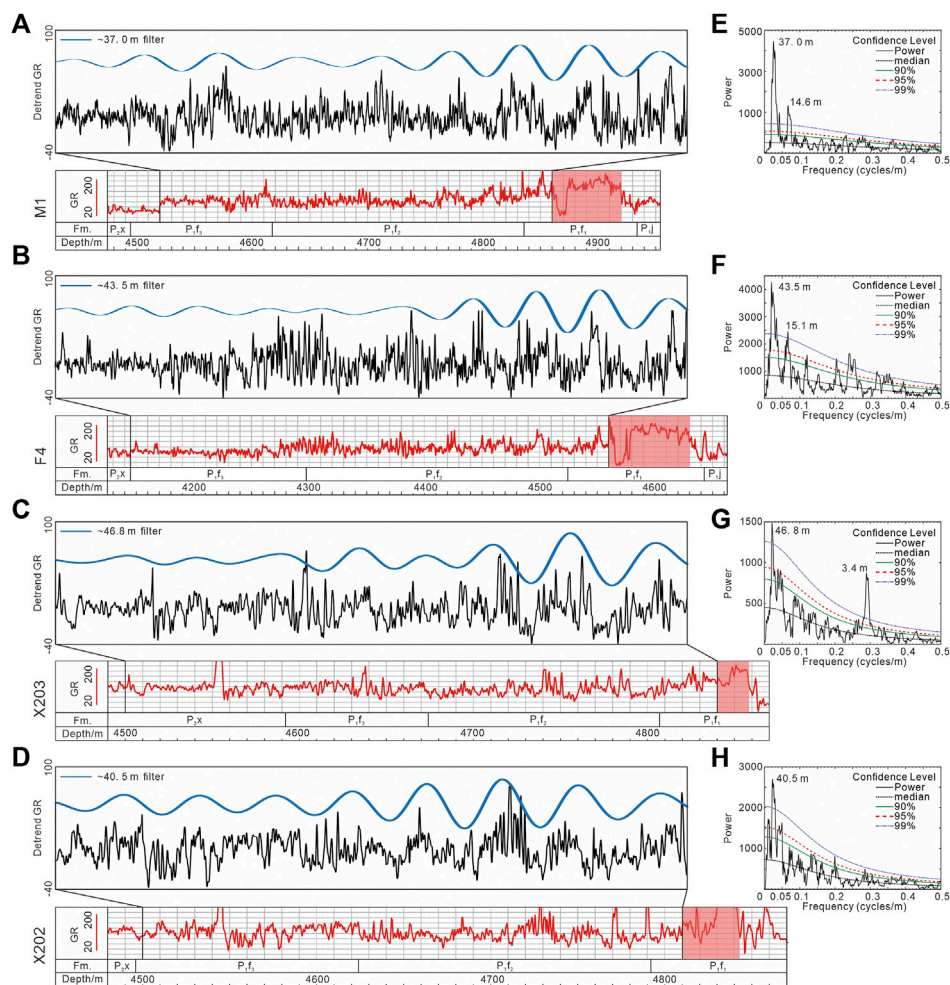


FIGURE 2

Spectral analysis and filter outputs of four wells: M1, F4, X203, and X202 (A–D). Raw NGR data (red curve) and standardized NGR data (black curve) after pretreatment of detrending and removing event perturbations and filter outputs (blue wave line) by isolating specific frequency. (E–H) The main filtered cycles with more than 99% confidence level of four sections were calculated and identified by the 2π multi-taper method (MTM) spectral estimator. The red shades in (A–D) represent the widespread and simultaneous volcanism in the lower member of Fengcheng Formation, which is as an anchored point for absolute time scale in this study.

distinguish mudstone from siltstone at a value of approximately 69 GAPI. 3) Resistivity (R_t) is a logs index used to measure the resistivity of the original strata, which could help to distinguish “calcareous” lithofacies from those of “dolomitic.” In general, “calcareous” is classified with an R_t value of 15–80 Ωm , while “dolomitic” is identified with a value higher than 80 Ωm . Detailed integrated logging characteristics of the different lithofacies are listed in Table 1.

4 Results

4.1 Times series analysis

The 2π multitaper (MTM) power spectrum of 4-wells NGR series shows significant peaks above 99% confidence level at wavelengths of 37.0 m, 14.6 m for M1, 43.5 m, 15.1 m for F4 and 46.8 m, 3.4 m for X203, and 40.5 m for X202 respectively (Figure 2).

Then Low-pass Gaussian filters were used to recognize and isolate the low-frequency and secular trend components through the entire NGR series, and the filter outputs of specific frequencies for targeted series intervals were shown above the detrended NGR curves (Figure 2). Nine cycles were identified in the Fengcheng Formation of F 4; those of the other wells were at least eight.

The correlation coefficient (COCO) approach can help estimate the most likely sedimentation rate, and the studied section and two representative wells, M1 and X203, were applied to this COCO approach. Three potential sedimentation rates at 3.5 cm/kyr, 9–12 cm/kyr, and 14–15 cm/kyr of M1 have null hypothesis (H_0) significant levels of less than 0.01, indicating the null hypothesis of no astronomical signal can be rejected at a 1% (H_0 value < 2–10). In other words, the significance level of the presence of an astronomical signal was 99%, but the sedimentation rate at 9–12 cm/kyr yields correlation coefficient values higher than 0.4, which were generally higher than those of the other two sedimentation rates (Figure 3A). Together, these two indices indicate that the most likely sedimentation rate of

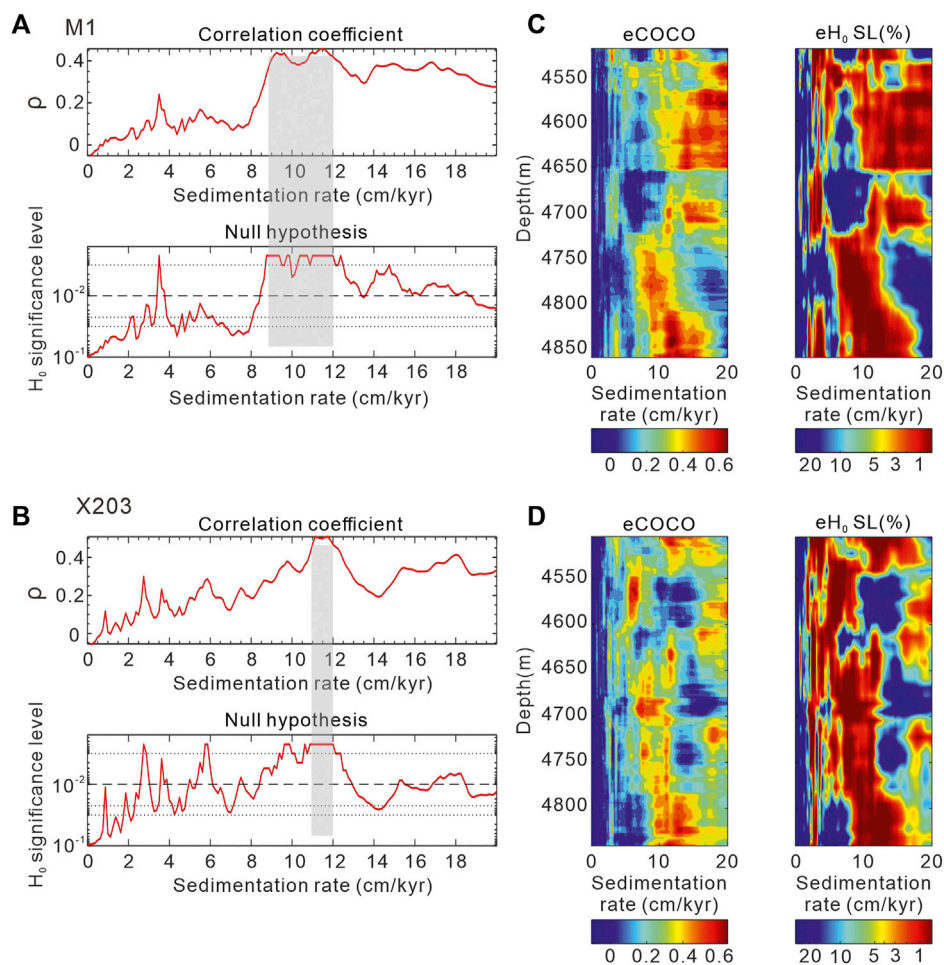


FIGURE 3

Sedimentation rate estimations of the Fengcheng Formation of wells M1 and X203 based on COCO and eCOCO analysis. (A,B) With the highest correlation coefficient value and smallest null hypothesis (H_0) significance level, the most likely sedimentation rates are 9–12 cm/kyr and 11–12 cm/kyr for M1 and X203 respectively. (C,D) Changes in sedimentation rates along the sections of both wells were demonstrated with the evolutionary correlation coefficient (eCOCO) map and the evolutionary null hypothesis significance level map.

M1 varies between 9 and 12 cm/kyr. The results of the COCO analysis of well X203 showed that the most likely sedimentation rate varies between 11 and 12 cm/kyr (Figure 3B). The evolutionary correlation coefficient (eCOCO) and evolutionary null hypothesis significance level (eH₀SL) maps show the change of the sedimentation rate through the data series (Figures 3C, D); a relatively stable sedimentation rate at 10–15 cm/kyr is significantly identified in the lower part of the targeted section with upwards reducing to 9–10 cm/kyr slowly, and at the top of the targeted section, the sedimentation rates are significantly increased to about 15 cm/kyr.

4.2 Astronomical tuning and floating astronomical time scale

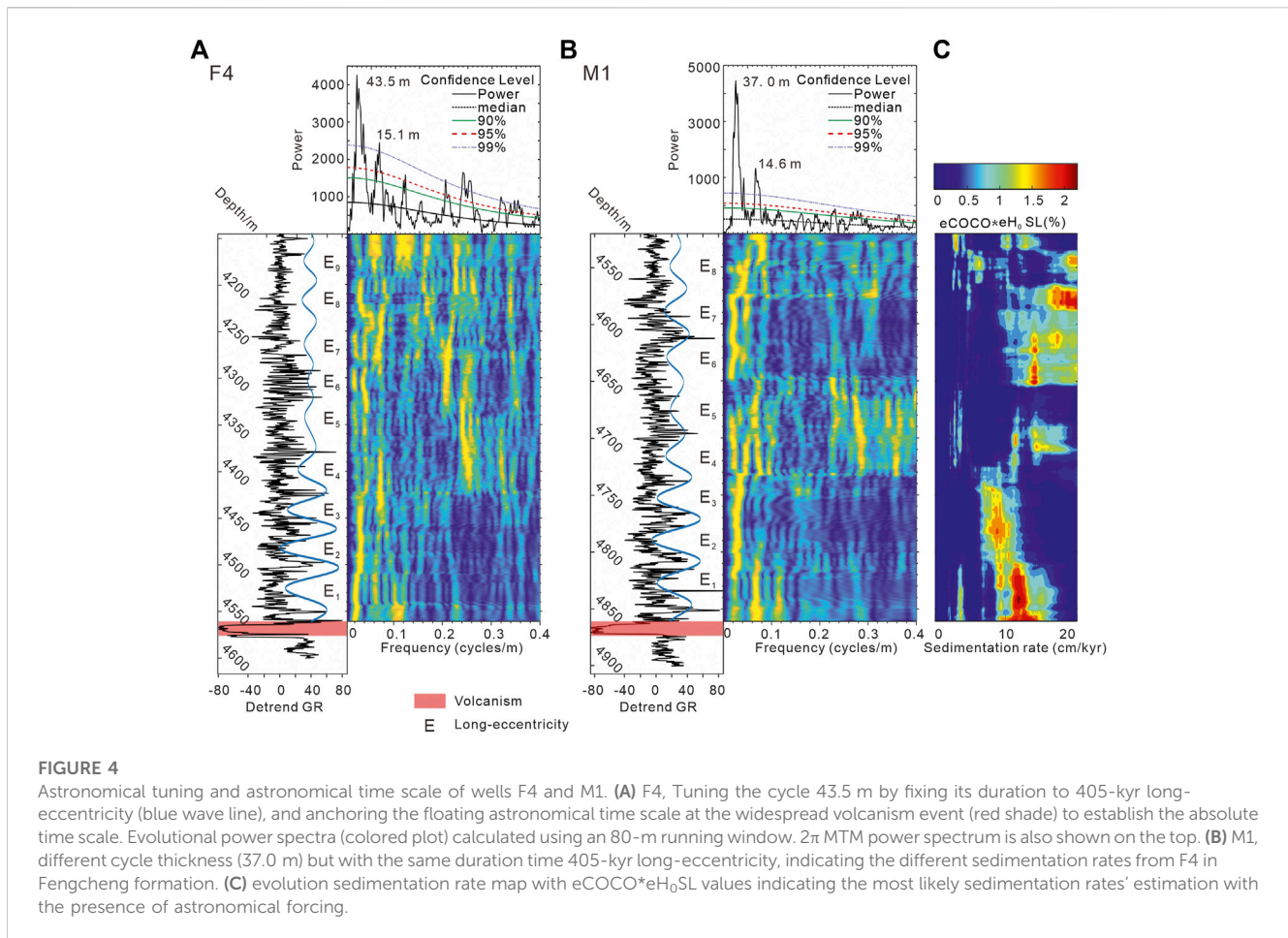
Based on both the filtered outputs of the NGR data series and the corresponding estimation of the most likely sedimentation rate, a simple calculation can be conducted by dividing the wavelength of the filtered output by the sedimentation rate, which generates the duration time of a single cycle. Taking wells M1 and X203 as

examples, with filtered outputs of 37 m/cycle and 46.8 m/cycle and sedimentation rates of 9–12 cm/kyr and 11–12 cm/kyr, the duration time of a single cyclicity is generated ranging between 308–412 kyr and 390–468 kyr respectively, and almost the same duration ranges were obtained from the other two NGR log data. Numerical models indicate that the ~405 kyr long-eccentricity cycles can be recognized through the Late Permian (Wu et al., 2013). Collectively, we tuned these filtered outputs extracted from several NGR data series by fixing the duration time of every single cycle to a 405 kyr long-eccentricity (Figure 4) and yield a ~3.6 Ma long floating astronomical time scale of (ATS) for the Fengcheng Formation in the northern Mahu Sag.

5 Discussion

5.1 Astrochronology of the Fengcheng Formation

An absolute astronomical time scale (ATS) can be constructed by anchoring a floating ATS to the absolute time (Li et al., 2019a).



Widespread volcanism in the lower Fengcheng Formation of the northern Mahu Sag was discovered by identification of the lithofacies based on log data series, marked by a combination of basalt and an underlying tuff layer, which are characterized by unusually low GR and unusually high GR values, respectively (Figures 2, A,B). The absolute astronomical time scale was constructed by anchoring the floating ATS to the U-Pb age of volcanism (~300 Ma) in the lower member of the Fengcheng Formation (Li et al., 2023). The common anchored time of the ATS and the same duration of cycles form an established isochronal framework of the northern Mahu Sag, by calibrating the beginning of the time series and the long-eccentricity cycles of adjacent wells.

Frequency ratio is a common approach to test whether the observed cycles in data series were formed by astronomical forcing (Hinnov, 2000). Except for the 405-kyr long eccentricity cycle, no other prominent astronomical cycles were discovered in the spectral analysis, such as short-eccentricity, obliquity, and precession (Figure 4). Therefore, we cannot use frequency ratios to calibrate the long eccentricity to tune other astronomical cycles. The results of the time series analysis show that the long-eccentricity cycles are remarkable in the lower part of the targeted Fengcheng Formation (Figures 4A, B), but upward ambiguous cycle signals complicate the interval, and the long-eccentricity cycle signals become less certain (with depth of 4300–4400 m of F4 in Figure 4A and 4650–4730 m for M1 in Figure 4B), which indicates more intense sedimentary perturbations. Based on both the evolutionary spectral analysis and

the evolutionary sedimentation rate map of M1 well (Figure 4), the intervals with clear and robust astronomical cycle signals have sedimentation rate estimations with stable variation and a high significance level. The sedimentation rate in the upper part of the Fengcheng Formation was higher than that in the lower part, as indicated by the estimation of the eCOCO*eH₀SL map (Figure 4C).

5.2 Sedimentary isochronal framework and spatial variation of lithofacies

Based on the absolute astronomical time scale of 12 wells in the northern Mahu Sag and the criterion of lithofacies' identification, a sedimentary isochronal framework involving the absolute time scale, distribution, and variation of lithofacies was constructed (Figure 5). Although the Fengcheng Formation has been recognized as having a heterogeneous lithology and sedimentary facies (Tang Y et al., 2021), this sedimentary isochronal framework provides an approach for investigating and describing the distribution and spatial variation of lithofacies.

Three crossing profiles were constructed within an isochronal framework to demonstrate the variation in lithofacies in the northern Mahu Sag. The two NE-SW trending profiles show variation in the lithofacies along the provenance direction (Figures 5A, B), and the NW-SE trending profile shows lithofacies' variation subvertical to the provenance direction

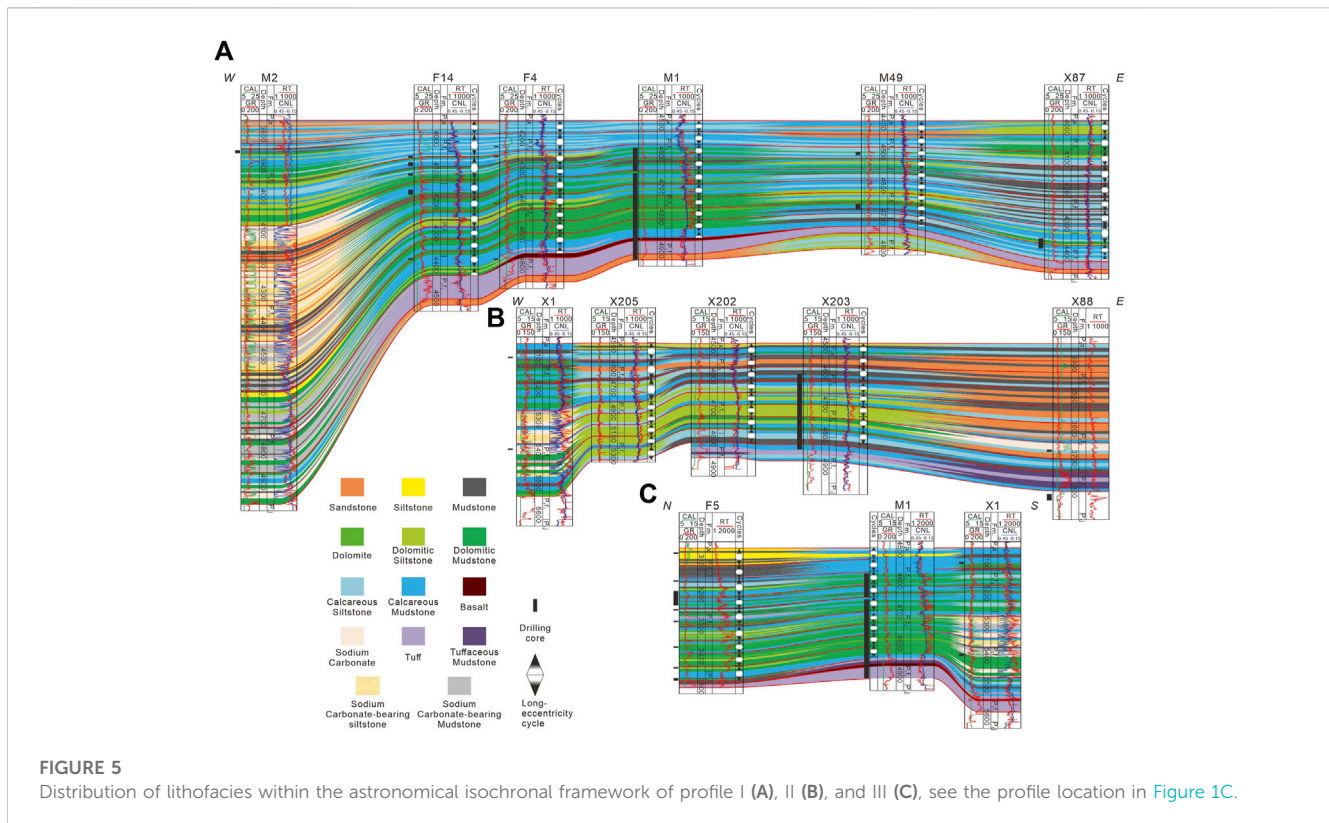


(Figure 5C). According to profile I, widespread volcanism occurred in the lower member of the Fengcheng Formation in the northern Mahu Sag and upward, the lithofacies were principally composed of calcareous and dolomitic mudstone and siltstone. The distinct facies change from the marginal fan to the central deep lake, especially in the middle member of the Fengcheng Formation. For example, in the M2 well, the facies changed from calcareous mudstone or siltstone in the marginal fan to dolomitic mudstone in the central deep lake environment and a large mass of sodium carbonate minerals emerged in the middle member of the Fengcheng Formation. In the upper Fengcheng Formation, the lithofacies consist of calcareous mudstone and siltstone, with small amounts of dolomitic mudstone and siltstone. The coarser grain size from the lower member to the upper member indicates a trend of the lake level gradually becoming shallower, especially the remarkable facies change in wells F14, F4, and M1 (Figure 5A), corresponding to the change in the sedimentation rate of the evolutionary correlation coefficient analysis (Figure 4). In addition, the lateral variations in lithofacies showed favorable continuity within the framework, which is consistent with the astronomical time scale. Profile II has a similar trend with profile I from the marginal to the central zone but reveals more distinct facies changes. In the middle member of the Fengcheng Formation, an apparent change in lithofacies from sandstone interbedded with mudstone to dolomitic siltstone is displayed, and the lithofacies upward become more complex, indicating more intense sedimentary perturbations. Well X1 in the central zone of the Mahu Sag also shows the accumulation of sodium carbonate minerals under deep lacustrine conditions.

Profile III demonstrates a direction vertical to the trend of profiles I and II, and reveals different variations of lithofacies' characteristics. The

lithofacies in profile III (Figure 5C) gradually changed vertically from dolomitic mudstone chiefly to interbedded dolomitic and calcareous mudstone and transformed into calcareous mudstone chiefly in the upper member. The lateral distribution of lithofacies revealed better continuity and stability than in profiles I and II. There are no prominent changes in lithofacies in the lower and middle parts of the Fengcheng Formation. However, there is a remarkable terrigenous supply from the NW to SE, as shown by the F5 well in the upper member of the Fengcheng Formation (Figure 5C), indicating that the lake level became shallow and sedimentary perturbations gradually intensified.

Among the three profiles, the lithofacies' identification results were consistent with the absolute astronomical time scale. In other words, based on the cyclostratigraphy, the correlation of lithofacies of the alkaline lacustrine deposits can be established. Therefore, the ATS is reliable and the lithofacies' distribution within the isochronal framework is effective for investigating the spatial variation of lithofacies of alkaline lacustrine deposits in the northern Mahu Sag, providing a reference for understanding the sedimentation process. Lateral continuity and variation contribute to the search for favorable intervals in the lithofacies. Dissolved pores in dolomites and microfractures associated with laminae can greatly contribute to the pore volume of dolomitic mudstones. Tuffaceous mudstones have plenty of dissolved pores in feldspars. Therefore, dolomitic and tuffaceous mudstones have been shown to have better resource potential (Tang et al., 2022). Dolomitic mudstones developed in the central and transitional zones corresponding to three long-eccentricity cycles in the middle member of the Fengcheng Formation. Tuffaceous mudstones are mainly developed in the lower member of the Fengcheng Formation in the marginal zone of the Mahu Sag. The factors controlling the lithofacies' distribution should be further investigated

in the future. This study goes beyond the demonstration of variations in lithofacies in Lower Permian alkaline lacustrine deposits through a cyclostratigraphy study and attempts to establish an approach to demonstrate lithofacies' framework in lacustrine deposits.

6 Conclusion

The alkaline lacustrine deposits of the Fengcheng Formation in the northern Mahu Sag record the sedimentary response of paleoclimatic change to astronomical forcing. Based on cyclostratigraphic analyses of the NGR, nine 405-kyr long-eccentricity cycles in the Fengcheng Formation were identified, and the absolute astronomical time scales could be established with the anchored point at ~300 Ma in the Lower member of the Fengcheng Formation. By calibrating the ATSS of different wells, an isochronal framework of the Fengcheng Formation was constructed for the northern Mahu Sag.

Combined with the identification of lithofacies from logging data, the lithofacies' correlation of alkaline lacustrine deposits was well established. The ATS is reliable and the distribution of the lithofacies within the isochronal framework is effective for investigating the spatial variation in the lithofacies of the alkaline lacustrine deposits in the northern Mahu Sag. Favorable lithofacies with high potential are well demonstrated in the spatio-temporal lateral lithofacies' framework. This study demonstrates an approach that can be used in the study of lithofacies in lacustrine deposits.

Data availability statement

The original contributions presented in the study are included in the article/supplementary material, further inquiries can be directed to the corresponding author.

References

- Burton, D., Woolf, K., and Sullivan, B. (2014). Lacustrine depositional environments in the green river formation, Uinta basin: Expression in outcrop and wireline logs. *AAPG Bull.* 98 (9), 1699–1715. doi:10.1306/03201413187
- Cantalejo, B., and Pickering, K. T. (2015). Orbital forcing as principal driver for fine-grained deep-marine siliciclastic sedimentation, Middle-Eocene Ainsa Basin, Spanish Pyrenees. *Paleogeogr. Paleoclimatol. Paleocol.* 421, 24–47. doi:10.1016/j.palaeo.2015.01.008
- Cao, J., Lei, D. W., Li, Y. W., Tang, Y., Abulimit, Chang, Q. S., et al. (2015). Ancient high-quality alkaline lacustrine source rocks discovered in the lower permian Fengcheng Formation, Junggar Basin. *Acta Pet. Sin.* 36 (07), 781–790. (in Chinese with English Abstract). doi:10.7623/syxb201507002
- Cao, J., Xia, L., Wang, T., Zhi, D., Tang, Y., and Li, W. (2020). An alkaline lake in the late paleozoic Ice age (LPIA): A review and new insights into paleoenvironment and petroleum geology. *Earth-Sci. Rev.* 202, 103091. doi:10.1016/j.earscirev.2020.103091
- Chen, S., Guo, Z., Pe-Piper, G., and Zhu, B. (2013). Late Paleozoic peperites in West Junggar, China, and how they constrain regional tectonic and palaeoenvironmental setting. *Gond. Res.* 23, 666–681. doi:10.1016/j.gr.2012.04.012
- Guo, P., Wen, H., Gibert, L., Jin, J., Wang, J., and Lei, H. (2021). Deposition and diagenesis of the Early Permian volcanic-related alkaline playa-lake dolomitic shales, NW Junggar Basin, NW China. *Mar. Pet. Geol.* 123, 104780. doi:10.1016/j.marpetgeo.2020.104780
- Han, Y., and Zhao, G. (2018). Final amalgamation of the tianshan and junggar orogenic collage in the southwestern central asian orogenic belt: Constraints on the closure of the paleo-Asian ocean. *Earth-Sci. Rev.* 186, 129–152. doi:10.1016/j.earscirev.2017.09.012
- Hinnov, L. A. (2013). Cyclostratigraphy and its revolutionizing applications in the Earth and planetary sciences. *Geol. Soc. Am. Bull.* 125 (11–12), 1703–1734. doi:10.1130/b30934.1
- Hinnov, L. A. (2000). New perspectives on orbitally forced stratigraphy. *Annu. Rev. Earth Planet. Sci.* 28, 419–475. doi:10.1146/annurev.earth.28.1.419
- Hu, S., Bai, B., Tao, S., Bian, C., Zhang, T., Chen, Y., et al. (2022). Heterogeneous geological conditions and differential enrichment of medium and high maturity continental shale oil in China. *Pet. Explor. Dev.* 49 (2), 257–271. doi:10.1016/s1876-3804(22)60022-3
- Huang, H., Gao, Y., Jones, M. M., Tao, H., Carroll, A. R., Ibarra, D. E., et al. (2020). Astronomical forcing of Middle Permian terrestrial climate recorded in a large paleolake in northwestern China. *Paleogeogr. Paleoclimatol. Paleocol.* 550, 109735. doi:10.1016/j.palaeo.2020.109735
- Huang, H., Gao, Y., Ma, C., Niu, L., Dong, T., Tian, X., et al. (2021). Astronomical constraints on the development of alkaline lake during the carboniferous-permian period in north pangea. *Glob. Planet. Change.* 207, 103681. doi:10.1016/j.gloplacha.2021.103681
- Jiang, C., Wang, G., Song, L., Huang, L., Wang, S., Zhang, Y., et al. (2023). Identification of fluid types and their implications for petroleum exploration in the shale oil reservoir: A case study of the Fengcheng Formation in the Mahu sag, Junggar Basin, northwest China. *Mar. Pet. Geol.* 147, 105996. doi:10.1016/j.marpetgeo.2022.105996
- Jin, Z., Zhu, R., Liang, X., and Shen, Y. (2021). Several issues worthy of attention in current lacustrine shale oil exploration and development. *Pet. Explor. Dev.* 48 (6), 1471–1484. doi:10.1016/s1876-3804(21)60303-8
- Li, D., He, D., Qi, X., and Zhang, N. (2015). How was the carboniferous balkhash–West Junggar remnant ocean filled and closed? Insights from the well tacan-1 strata in the tacheng basin, NW China. *Gond. Res.* 27 (1), 342–362. doi:10.1016/j.gr.2013.10.003
- Li, M., Hinnov, L. A., Huang, C., and Ogg, J. G. (2018a). Sedimentary noise and sea levels linked to land-ocean water exchange and obliquity forcing. *Nat. Commun.* 9 (1), 1004. doi:10.1038/s41467-018-03454-y

Author contributions

YT resources and project administration; WH resources and project administration; RW resources; HR resources; ZJ project administration; ZY writing—original draft and data processing. YZ supervision, conceptualization, writing, review, and editing. All authors contributed to the article and approved the submitted version.

Funding

This research is supported by the Natural Science Foundation of China (NSFC) Project given to Prof. Zhaojie Guo (No. 42090021).

Conflict of interest

Authors YT, WH, RW, and HR were employed by PetroChina Xinjiang Oilfield Company.

The remaining authors declare that the research was conducted in the absence of any commercial or financial relationships that could be construed as a potential conflict of interest.

Publisher's note

All claims expressed in this article are solely those of the authors and do not necessarily represent those of their affiliated organizations, or those of the publisher, the editors and the reviewers. Any product that may be evaluated in this article, or claim that may be made by its manufacturer, is not guaranteed or endorsed by the publisher.

- Li, M., Hinnov, L., and Kump, L. (2019a). Acycle: Time-series analysis software for paleoclimate research and education. *Comput. Geosciences* 127, 12–22. doi:10.1016/j.cageo.2019.02.011
- Li, M., Kump, L. R., Hinnov, L. A., and Mann, M. E. (2018b). Tracking variable sedimentation rates and astronomical forcing in Phanerozoic paleoclimate proxy series with evolutionary correlation coefficients and hypothesis testing. *Earth Planet. Sci. Lett.* 501, 165–179. doi:10.1016/j.epsl.2018.08.041
- Li, M., Ma, X. X., Jiang, Q. G., Li, Z. M., Pang, X. Q., Zhang, C. T., et al. (2019b). Enlightenment from formation conditions and enrichment characteristics of marine shale oil in north America. *Pet. Geol. Recovery Effic.* 26 (01), 13–28. (in Chinese with English Abstract). doi:10.13673/j.cnki.cn37-1359/te.2019.01.002
- Li, W., Zhang, Y., He, W., and Tang, Y. (2023). Subaqueous felsic volcanic sequence and its contribution to the ancient alkaline lacustrine deposits in the Mahu Sag, Junggar Basin, NW China. *Geol. J.* 2023, 4812. doi:10.1002/gj.4812
- Liang, Y., Zhang, Y., Chen, S., Guo, Z., and Tang, W. (2020). Controls of a strike-slip fault system on the tectonic inversion of the Mahu depression at the northwestern margin of the Junggar Basin, NW China. *J. Asian Earth Sci.* 198, 104229. doi:10.1016/j.jseas.2020.104229
- Liu, B., Han, B.-F., Chen, J.-F., Ren, R., Zheng, B., Wang, Z.-Z., et al. (2017). Closure time of the junggar-balkhash ocean: Constraints from late paleozoic volcano-sedimentary sequences in the barleik mountains, West Junggar, NW China. *Tectonics* 36 (12), 2823–2845. doi:10.1002/2017tc004606
- Liu, Y., Wang, X., Wu, K., Chen, S., Shi, Z., and Yao, W. (2019). Late Carboniferous seismic and volcanic record in the northwestern margin of the Junggar Basin: Implication for the tectonic setting of the West Junggar. *Gond. Res.* 71, 49–75. doi:10.1016/j.gr.2019.01.013
- Montañez, I. P., and Poulsen, C. J. (2013). The late paleozoic Ice age: An evolving paradigm. *Annu. Rev. Earth Planet. Sci.* 41 (1), 629–656. doi:10.1146/annurev.earth.031208.100118
- Ni, M., Zhang, Y., Tang, Y., and He, W. (2023). Distribution characteristics of organic matter in the Fengcheng Formation in Mahu sag, Junggar Basin: Implications for hydrocarbon generation model in alkaline lacustrine deposition. *Front. Earth Sci.* 11. doi:10.3389/feart.2023.1218788
- Pecoraino, G., D'Alessandro, W., and Inguaggiato, S. (2015). The other side of the coin: Geochemistry of alkaline lakes in volcanic areas. *Volcan. Lakes* 2015, 219–237. doi:10.1007/978-3-642-36833-2_9
- Qian, Y., Zou, Y., Zhao, X., Chang, Q., He, W., and Huang, L. (2022). Full core analysis and petroleum geological significance of permian Fengcheng Formation in well-MY1, Mahu sag. *Petroleum Reserv. Eval. Dev.* 12 (1), 204–214. (in Chinese with English Abstract). doi:10.13809/j.cnki.cn32-1825/te.2022.01.018
- Schnyder, J., Ruffell, A., Deconinck, J.-F., and Baudin, F. (2006). Conjunctive use of spectral gamma-ray logs and clay mineralogy in defining late Jurassic–early Cretaceous palaeoclimate change (Dorset, U.K.). *Paleogeogr. Paleoclimatol. Paleoecol.* 229 (4), 303–320. doi:10.1016/j.palaeo.2005.06.027
- Sha, J., Olsen, P. E., Pan, Y., Xu, D., Wang, Y., Zhang, X., et al. (2015). Triassic–Jurassic climate in continental high-latitude Asia was dominated by obliquity-paced variations (Junggar Basin, Urumqi, China). *Proc. Natl. Acad. Sci. U. S. A.* 112 (12), 3624–3629. doi:10.1073/pnas.1501137112
- Smith, M. E., and Carroll, A. R. (2015). *Stratigraphy and paleolimnology of the green river formation*. western USA: Springer.
- Tang, W., Zhang, Y., Pe-Piper, G., Piper, D. J. W., Guo, Z., and Li, W. (2021). Permian to early triassic tectono-sedimentary evolution of the Mahu sag, Junggar Basin, Western China: Sedimentological implications of the transition from rifting to tectonic inversion. *Mar. Pet. Geol.* 123, 104730. doi:10.1016/j.marpetgeo.2020.104730
- Tang, Y., Cao, J., He, W. J., Guo, X. G., Zhao, K. B., and Li, W. W. (2021). Discovery of shale oil in alkaline lacustrine basins: The late paleozoic Fengcheng Formation, Mahu sag, Junggar Basin, China. *Pet. Sci.* 18, 1281–1293. doi:10.1016/j.petsci.2021.04.001
- Tang, Y., He, W., Zheng, M., Chang, Q., Jin, Z., and Li, J. (2022). Shale lithofacies and its effect on reservoir formation in Lower Permian alkaline lacustrine Fengcheng Formation, Junggar Basin, NW China. *Front. Earth Sci.* 10. doi:10.3389/feart.2022.930890
- Wang, M., Chen, H., Huang, C., Kemp, D. B., Xu, T., Zhang, H., et al. (2020). Astronomical forcing and sedimentary noise modeling of lake-level changes in the Paleogene Dongpu Depression of North China. *Earth Planet. Sci. Lett.* 535, 116116. doi:10.1016/j.epsl.2020.116116
- Wang, T., Cao, J., Carroll, A. R., Zhi, D., Tang, Y., Wang, X., et al. (2020). Oldest preserved sodium carbonate evaporite: Late paleozoic Fengcheng Formation, Junggar Basin, NW China. *GSA Bull.* 133 (7–8), 1465–1482. doi:10.1130/b35727.1
- Warren, J. K. (2010). Evaporites through time: Tectonic, climatic and eustatic controls in marine and nonmarine deposits. *Earth-Science Rev.* 98 (3–4), 217–268. doi:10.1016/j.earscirev.2009.11.004
- Wu, H., Zhang, S., Hinnov, L. A., Jiang, G., Feng, Q., Li, H., et al. (2013). Time-calibrated Milankovitch cycles for the late permian. *Nat. Commun.* 4, 2452. doi:10.1038/ncomms3452
- Xia, L., Cao, J., Jin, J., Xiang, B., Ma, W., and Wang, T. (2022). Response of nitrogen isotopes to paleo-environment and organic carbon accumulation in a Late Paleozoic alkaline lake, Junggar Basin. *Chem. Geol.* 602, 120884. doi:10.1016/j.chemgeo.2022.120884
- Yu, K., Cao, Y., Qiu, L., and Sun, P. (2019). Depositional environments in an arid, closed basin and their implications for oil and gas exploration: The lower Permian Fengcheng Formation in the Mahu sag, northwestern Junggar Basin, China. *AAPG Bull.* 103 (9), 2073–2115. doi:10.1306/01301917414
- Yu, K., Cao, Y., Qiu, L., Sun, P., Jia, X., and Wan, M. (2018). Geochemical characteristics and origin of sodium carbonates in a closed alkaline basin: The lower permian Fengcheng Formation in the Mahu sag, northwestern Junggar Basin, China. *Paleogeogr. Paleoclimatol. Paleoecol.* 511, 506–531. doi:10.1016/j.palaeo.2018.09.015
- Yu, Y., Wang, X., Rao, G., and Wang, R. (2016). Mesozoic reactivated transpressional structures and multi-stage tectonic deformation along the Hong-Che fault zone in the northwestern Junggar Basin, NW China. *Tectonophysics* 679, 156–168. doi:10.1016/j.tecto.2016.04.039
- Zhang, X., Zhao, G., Sun, M., Eizenhöfer, P. R., Han, Y., Hou, W., et al. (2016). Tectonic evolution from subduction to arc-continent collision of the Junggar ocean: Constraints from U-Pb dating and Hf isotopes of detrital zircons from the North Tianshan belt, NW China. *Geol. Soc. Am. Bull.* 128 (3–4), 644–660. doi:10.1130/b31230.1
- Zhang, Y., Pe-Piper, G., Piper, D. J. W., and Guo, Z. (2013). Early Carboniferous collision of the Kalamaili orogenic belt, North Xinjiang, and its implications: Evidence from molasse deposits. *Geol. Soc. Am. Bull.* 125 (5–6), 932–944. doi:10.1130/b30779.1
- Zhi, D. M., Tang, Y., Zheng, M. L., Xu, Y., Cao, J., Ding, J., et al. (2019). Geological characteristics and accumulation controlling factors of shale reservoirs in Fengcheng Formation, Mahu sag, Junggar Basin. *China Pet. explor.* 24 (05), 615–623. (in Chinese with English Abstract). doi:10.3969/j.issn.1672-7703.2019.05.008